Biochemical and Biophysical Research Communications 402 (2010) 94–98

Contents lists available at ScienceDirect

Biochemical and Biophysical Research Communications

journal homepage: www.elsevier.com/locate/ybbrc

Evodiamine as a novel antagonist of aryl hydrocarbon receptor

Hui Yu [a,b,1], Yongjiu Tu [a,1], Chun Zhang [a], Xia Fan [a], Xi Wang [a], Zhanli Wang [c], Huaping Liang [a,*]

[a] State Key Laboratory of Trauma, Burns, and Combined Injury, Department 1, Research Institute of Surgery, Daping Hospital, The Third Military Medical University, Chongqing 400042, China
[b] Department of Laboratory Medicine, The Affiliated Tenth People's Hospital, Tongji University, Shanghai 200072, China
[c] College of Pharmaceutical Science, Zhejiang University of Technology, Hangzhou 310014, China

ARTICLE INFO

Article history:
Received 22 September 2010
Available online 1 October 2010

Keywords:
Aryl hydrocarbon receptor
Evodiamine
Docking
Homology modeling
Antagonist

ABSTRACT

Evodiamine, the major bioactive alkaloid isolated from Wu-Chu-Yu, has been shown to interact with a wide variety of proteins and modify their expression and activities. In this study, we investigated the interaction between evodiamine and the aryl hydrocarbon receptor (AhR). Molecular modeling results revealed that evodiamine directly interacted with the AhR. Cytosolic receptor binding assay also provided the evidence that evodiamine could interact with the AhR with the K_i value of 28.4 ± 4.9 nM. In addition, we observed that evodiamine suppressed the 2,3,7,8-tetrachlorodibenzo-*p*-dioxin (TCDD) induced nuclear translocation of the AhR and the expression of CYP1A1 dose-dependently. These results suggested that evodiamine was able to bind to the AhR as ligand and exhibit antagonistic effects.

1. Introduction

Evodiamine, the major bioactive alkaloid isolated and purified from Chinese herbal drug named Wu-Chu-Yu, has been reported to exhibit anti-inflammation, anti-tumor growth and anti-angiogenic activity [1]. Accumulating evidence suggests that evodiamine modulates various targets either through direct interaction or through modulation of gene expression, including vanilloid receptor, Bcl-2 and other gene products linked with cell survival, proliferation, invasion, and angiogenesis [2].

The AhR, a ligand-dependent transcription factor, is a member of the Per-Arnt–Sim family that has been detected in most cell and tissue types [3]. AhR includes a ligand binding domain (LBD) and interacts directly with specific ligands. The best-characterised AhR agonist is TCDD, which binds to the AhR with the highest affinity of all known compounds. Other agonists can be found endogenously and in the diet [4,5]. Following agonist binding, the AhR translocates to the nucleus, forms a heterodimer with aryl hydrocarbon receptor nuclear transporter protein (ARNT), and modulate the expression of a number of genes, including cytochrome P450 1A1, 1A2, 1B1, glutathione S transferase M (GSTM), aldehyde dehydrogenase and oncogenes [6–9]. Moreover, some natural compounds have been reported to interact with the AhR and induce or inhibit the AhR transformation [10–14].

In this study, we investigated the specific interaction of evodiamine with AhR using computational approaches, and the interaction mechanism was discussed. We also investigated the inhibitory effect of evodiamine on the specific binding between the AhR and TCDD using cytosolic AhR binding assay. Moreover, we evaluated the antagonistic effects of evodiamine on the transformation of the AhR and its downstream events. We showed for the first time that evodiamine interacted with the AhR and was a potent antagonist of the AhR.

2. Materials and methods

2.1. Materials

TCDD (purity 99%) and [^{3}H]–TCDD (specific activity 33 Ci/mmol) were purchased from Anal-tech Science Limited (ShenZhen, China). Evodiamine (purity 99%) was purchased from Xi'an Guanyu Biotechnology Company Limited (Xi'an, China). All ligands were dissolved in DMSO. The DMSO concentration in the cell culture medium was below 0.1%. RPMI-1640 medium and fetal calf serum were purchased from Gibco BRL (Gaithersburg, Maryland, USA). DMSO was purchased from Sigma–Aldrich (St Louis, Missouri, USA). The following primary antibodies were used in this study: AhR, CYP1A1 (Santa Cruz Biotechnology, Santa Cruz, California, USA).

2.2. Homology modeling

We selected the PAS domain structure of hypoxia-inducible factor 2α (Hif-2α) (PDB code: 2A24) as the 3D coordinate template for the homology modeling of human AhR-LBD [15]. The primary amino acid sequence of the AhR-LBD (Genbank: NP_001612) was

* Corresponding author. Fax: +86 23 68757404.
E-mail address: huaping_liang@yahoo.com.cn (H. Liang).
[1] These authors contributed equally to this study.

0006-291X/$ - see front matter © 2010 Elsevier Inc. All rights reserved.
doi:10.1016/j.bbrc.2010.09.122

aligned with that of the template using Clustal W [16] with default settings. The gap penalties used were a gap opening penalty of ten and a gap extension penalty of 0.05. Three-dimensional model of the human AhR-LBD was constructed based on the structure of template using program Modeller. The entire model was globally energy minimized in the presence of explicit solvent model TIP3P water using the CHARMm program. The obtained structure was evaluated with the Verify3D programs.

2.3. Molecular docking

The human AhR-LBD model was used as a template for docking experiments with the ligands. The eHiTS software package was used for flexible docking [17]. The ligand was docked to the AhR-LBD model using the accuracy mode of docking (accuracy set to six) and scored with eHiTS Score, which is included in the eHiTS software package.

2.4. Cytosolic receptor binding assay

Wistar rats were purchased from third military medical university (Chongqing, China). The animals were housed in cages under standard laboratory conditions (24 °C, 60% humidity, 12 h dark/light cycle) and were given 3 days to adapt to standard laboratory conditions. These animals were used for cytosol preparation following liver perfusion. Liver cytosol from Wistar rats was prepared as previously described [18]. The IC_{50} and K_i values for competitive receptor binding affinities were determined using frozen rat hapatic cytosol (2 mg protein/ml) and the hydroxyapatite (HAP) procedure essentially as described using 1 nM [^{3}H]–TCDD as the radioligand [19]. Different concentrations of evodiamine or unlabled TCDD were used to determine displacement curves. The IC_{50} values were defined as the concentrations required to displace 50% of the [^{3}H]–TCDD and were determined from a probit plot of the percentage of [^{3}H]–TCDD bound versus log concentrations of the ligand. K_i values were determined by the methods of Cheng and Prusoff [20].

2.5. Cell culture and chemical treatment

Human Lovo cells were derived from the American Type Culture Collection (ATCC, Rockville, MD). Cells were maintained in RPMI-1640 medium containing 10% heat-inactive fetal bovine serum, 100 U/ml penicillin and 100 μg/ml streptomycin in a humidified incubator at 37 °C in 5% CO_2. 0.1 μM TCDD, different concentrations of evodiamine, and TCDD plus evodiamine were dissolved in DMSO (0.1%) and added to the culture dishes when the cells reached 70% confluence. Cells were harvested 24 h after chemical treatment.

2.6. Immunocytochemistry

After different chemical treatment, Lovo cells were then fixed in 4% paraformaldehyde for 30 min, blocked with 5% bovine serum albumin (BSA), stained with rabbit polyclonal anti-AhR (1:100 dilution) overnight at 4 °C. Subsequently, these cells were incubated with FITC-conjugated mouse anti-rabbit antibody (1:200) for 1 h. Cell nuclei was stained with 10 mg/ml DAPI and representative photographs were obtained under a laser confocal scanning microscope.

2.7. Real-time PCR

Total RNA from harvested human Lovo cells was extracted with TRIzol reagent (Invitrogen) according to the manufacturer's instructions. Quantitative real-time PCR analysis was performed by LightCycler (Roche) and SYBR RT-PCR kit (Takara, Dalian, China). The following primer sets were utilized: CYP1A1 FP 5′-TCC TTG TGA TCC CAG GCT C-3′, CYP1A1 RP 5′-CCA GGT GCG GGT TCT TT-3′, GAPDH FP 5′-GGG AAA CTG TGG CGT GAT-3′, GAPDH RP 5′-GAG TGG GTG TCG CTG TTG A-3′. Data were normalized by the level of GAPDH expression in each sample.

2.8. Western blot assay

Lovo cells were harvested and washed twice in ice-cold PBS. The cells were lysed with lysis buffer, then centrifuged at 13,000*g* for 15 min at 4 °C. The protein concentration was determined by a BCA protein assay kit. Protein was loaded onto SDS–PAGE gel and electro-transferred to polyvinylidene fluoride membranes. After being blocked with 5% non-fat milk, the membranes were incubated with mouse monoclonal anti-CYP1A1 followed by horseradish peroxidase conjugated rabbit anti-mouse secondary antibody. Finally, the membranes were visualized with an enhanced chemiluminescence kit.

2.9. Statistical analysis

All the experiments were carried out in triplicate, and the results are expressed as means ± SD. Statistical significance was determined by performing ANOVA using Student's *t*-test.

3. Results and discussion

3.1. Homology modeling of the human AhR-LBD

To construct the homology model of the human AhR-LBD, sequence alignments of the human AhR-LBD and the template were carried out (Fig. S1). The sequence identity between two proteins is low (27%). However, there is a high structural conservation of the α and β folds [21]. Therefore, we selected the PAS domain structure of Hif-2α for generating a 3D model of the human AhR-LBD based on its closest similarity in this region. The homology model of the human AhR-LBD was obtained using the primary amino acid sequence [283–390] of the human AhR (Fig. 1). The refined homology model was then geometrically corrected so that all of the residues were in sterically allowed regions of the Ramachandran plot (Fig. S2). Moreover, the Verify3D evaluation was also performed, the overall self-compatibility scores for the predicted structures were all above the expected values (Fig. S3). Our results indicated that the predicted model was reliable.

Fig. 1. Homology model of the human AhR-LBD with the protein backbone displayed as ribbon and colored by secondary structure (Discovery Studio Visualizer 2.5, Accelrys).

3.2. Detection of binding between the AhR-LBD and evodiamine by molecular docking

For the purpose of obtaining evidences that evodiamine binds to AhR-LBD, computational docking studies were performed using the human AhR-LBD model. To validate the docking method, we first applied our technique to the rebuilding of the TCDD–AhR complex by docking the TCDD into the binding pocket of AhR-LBD model (Fig. 2A). The result demonstrated that the predicted docking orientation of the TCDD was in excellent agreement with other studies [21]. To further validate our docking method, we also studied the binding of structurally diverse molecule pinocembrin to the AhR-LBD model (Fig. 2B). We observed that the 2-phenyl ring of pinocembrin allocated in the small hydrophobic cleft surrounded by residues Phe281, Leu309, Leu347 and Val363. Moreover, the hydroxyl group of pinocembrin established a hydrogen bond with the side chain of Ser365. These results were consistent with other studies [21]. These docking results confirmed that our AhR-LBD homology model was reasonable, and the docking method was reliable for the determination of the interactions between AhR-LBD and ligands. Evodiamine was then docked into the AhR-LBD model. The predicted binding mode of evodiamine is shown in Fig. 2C. In this model, similarity in binding pocket was observed when compared with TCDD and pinocembrin. However, it became obvious that a series of hydrophobic residues involved in complex formation: Phe285, Phe295, Gly304, Val307, Leu308, Ile325, Cys333, Met348, Val363, and Ser365. Hydrogen bonding did not appear to be as significant as it was with TCDD and pinocembrin. Interestingly, it has been proposed that the potent AhR agonists docked into the binding pockets in a similar orientation, establishing hydrogen bond interactions with protein residues facing the binding cavity [21]. By comparing the binding pattern of TCDD and evodiamine to the AhR binding pocket, we therefore suppose that TCDD and evodiamine may have differential effects on AhR activity.

We, next, analyzed the binding affinity of evodiamine with the AhR by docking score analysis. Results indicated that the score values of compounds ranked in the order of pinocembrin > evodiamine > TCDD. Because smaller score value means stronger affinity, evodiamine showed the higher affinity with the AhR than pinocembrin, as estimated by the docking score calculations of the ligand and protein complexes. It was previously demonstrated that pinocembrin inhibited TCDD binding to the AhR [11,12]. We therefore suppose that evodiamine also competitively inhibited TCDD binding to the AhR.

Taken together, these results implicated that evodiamine possibly bound to the binding site of the AhR and might act as competitive antagonist of the AhR, but not agonist. Docking orientation of TCDD, pinocembrin and evodiamine into the human AhR-LBD binding pocket was shown in Fig. S4.

3.3. Effects of evodiamine on binding between the cytosolic AhR and [^{3}H]–TCDD

To further confirm the above hypothesis, effects of evodiamine on binding between the cytosolic AhR and [^{3}H]–TCDD were exam-

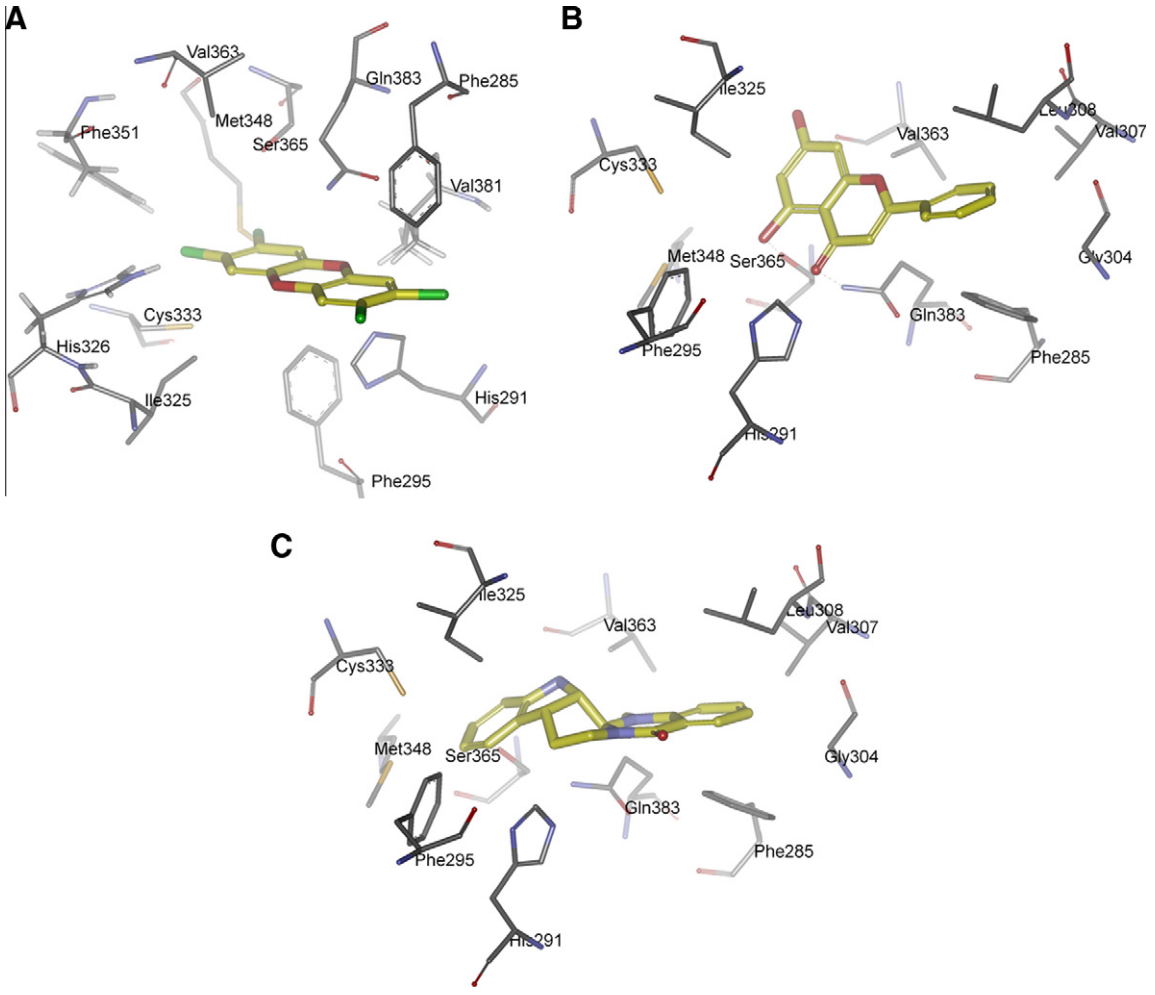

Fig. 2. Docking orientation of TCDD (A), pinocembrin (B) and evodiamine (C) respectively into the human AhR-LBD binding pocket.

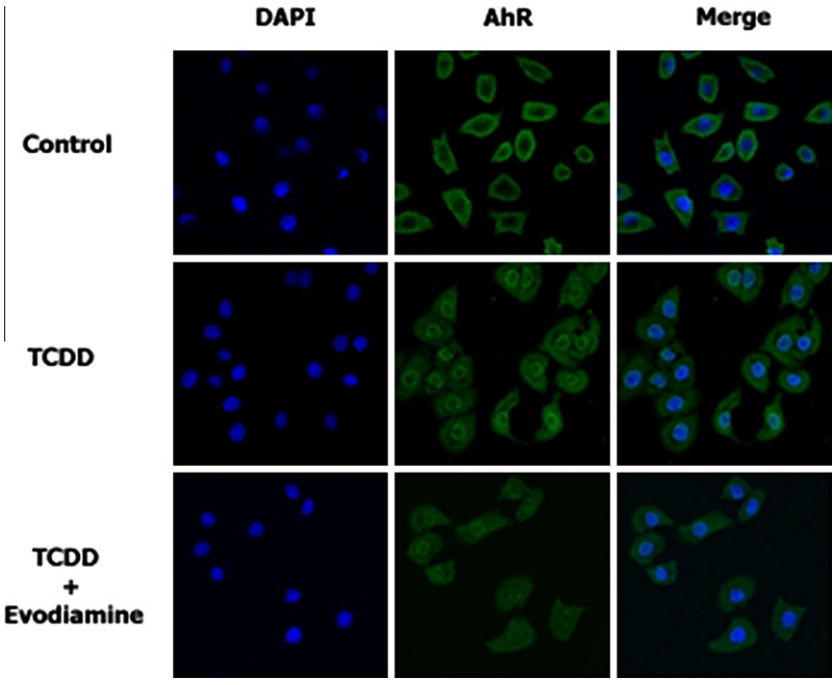

Fig. 3. Nuclear localization of the AhR in Lovo cells.

Table 1
Effects of evodiamine on the AhR induced CYP1A1 gene expression in Lovo cells[a].

Treatment	Concentration (μM)	CYP1A1 mRNA (10^{-4})
DMSO	–	8.5 ± 1.6
TCDD	0.1	14.8 ± 2.9[b]
Evodiamine	60	1.6 ± 0.2[c]
Evodiamine	30	3.8 ± 0.4[c]
Evodiamine	15	6.9 ± 1.0
TCDD + Evodiamine	0.1 + 60	9.1 ± 1.4[d]
TCDD + Evodiamine	0.1 + 30	10.5 ± 1.2[d]
TCDD + Evodiamine	0.1 + 15	12.5 ± 1.9

[a] Lovo cells were treated with 0.1 μM TCDD, 15–60 μM evodiamine in the presence or absence of 0.1 μM TCDD for 24 h; mRNA was isolated and quantitated by real-time RT-PCR (relative to GAPDH mRNA) as described under section 2. The results are expressed as mean ± SD for at least three determinations for each data point.
[b] Significantly higher ($p < 0.05$) than that in cells treated with DMSO alone.
[c] Significantly lower ($p < 0.01$) than that in cells treated with DMSO alone.
[d] Significantly lower ($p < 0.05$) than that in cells treated with TCDD alone.

ined by competitive ligand binding assay. Firstly, the competitive binding assay was validated and unlabelled TCDD was used to displace [^{3}H]–TCDD with the IC_{50} value of 1.71 ± 0.3 nM. This value is comparable to other studies [20], which confirmed that the conditions under which the displacement experiment was conducted were reliable. Then, the dose-dependent displacement of [^{3}H]–TCDD by evodiamine was determined. As the results, evodiamine inhibited the specific binding of [^{3}H]–TCDD to the AhR with an IC_{50} value of 44.8 ± 6.5 nM, which was in agreement with our docking studies. The corresponding K_i value calculated for evodiamine was 28.4 ± 4.9 nM.

3.4. Effects of evodiamine on nuclear translocation of the AhR

Since evodiamine competitively inhibited [^{3}H]–TCDD binding to the AhR, we further examined whether evodiamine could act as agonist or antagonist of the AhR. Confocal microscopy showed that TCDD (0.1 μM) promoted nuclear translocation of the AhR from cytosol after 4 h of exposure (Fig. 3). However, cotreatment with evodiamine (60 μM) strongly inhibited TCDD-induced nuclear translocation of the AhR in Lovo cells (Fig. 3), indicating that evodiamine acts as an antagonist of the AhR.

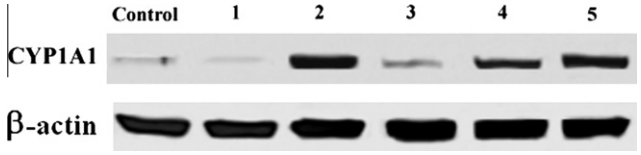

Fig. 4. Western blot showing the AhR induced CYP1A1 protein expression in Lovo cells. (1) 60 μM evodiamine; (2) 0.1 μM TCDD; (3) 60 μM evodiamine + 0.1 μM TCDD; (4) 30 μM evodiamine + 0.1 μM TCDD; (5) 15 μM evodiamine + 0.1 μM TCDD.

3.5. Effects of evodiamine on the AhR induced CYP1A1 gene and protein expression

The induction of CYP1A1 is well characterised as a measure of AhR agonism. To further confirm that evodiamine can act as an AhR antagonist, effects of evodiamine on AhR induced CYP1A1 gene and protein expression was measured. The results in Table 1 summarized the effects of compounds on CYP1A1 mRNA levels in Lovo cells. TCDD activated CYP1A1 in an AhR dependent manner. However, cotreatment with evodiamine inhibited TCDD-induced CYP1A1 mRNA levels in a dose-dependent manner. Furthermore, evodiamine suppressed the CYP1A1 protein expression in cultured Lovo cells, confirming its status as the AhR antagonist (Fig. 4).

Acknowledgments

This study was supported by grants from the National High Technology Research and Development Program (“863” Program) of China (No. 2008AA02Z440), the National Basic Research Program of China (No. 2005CB522602), the National Natural Science Foundation of China (No. 20902068) and Project of State Key Laboratory of Trauma, Burns, and Combined Injury (No. SKLZZ200802).

Appendix A. Supplementary data

Supplementary data associated with this article can be found, in the online version, at doi:10.1016/j.bbrc.2010.09.122.

References

[1] Y. Kano, Q. Zong, K. Komatsu, Pharmacological properties of galenical preparation. XIV. Body temperature retaining effect the Chinese traditional medicine, "Goshuyu-to" and component crude drugs, Chem. Pharm. Bull. 39 (1991) 690–692.
[2] X.F. Fei, B.X. Wang, T.J. Li, S. Yashiro, M. Minami, D.J. Xing, T. Ikejima, Evodiamine, a constituent of evodiae fructus, induces antiproliferating effects in tumor cells, Cancer Sci. 94 (2003) 92–98.
[3] M.E. Hahn, The aryl hydrocarbon receptor: a comparative perspective, Comp. Biochem. Physiol. 121 (1998) 23–53.
[4] C.J. Sinal, R.J. Bend, Aryl hydrocarbon receptor-dependent induction of Cyp1a1 by bilirubin in mouse hepatatoma hepa 1c1c7 cells, Mol. Pharmacol. 52 (1997) 590–599.
[5] S. Heath-Pagliuso, W.J. Rogers, K. Tullis, S.D. Seidel, P.H. Cenijn, A. Brouwer, M.S. Denison, Activation of the Ah receptor by tryptophan and tryptophan metabolites, Biochemistry 37 (1998) 11508–11515.
[6] K. Kawajiri, Y. Fujii-Kuriyama, Cytochrome P450 gene regulation and physiological functions mediated by the aryl hydrocarbon receptor, Arch. Biochem. Biophys. 464 (2007) 207–212.
[7] D. Brauze, M. Widerak, J. Cwykiel, K. Szyfter, W. Baer-Dubowska, The effect of aryl hydrocarbon receptor ligands on the expression of AhR, AhRR, ARNT, Hif1alpha, CYP1A1 and NQO1 genes in rat liver, Toxicol. Lett. 167 (2006) 212–220.
[8] T.H. Rushmore, R.G. King, E.K. Paulson, C.B. Pickett, Regulation of glutathione S-transferase Ya subunit gene expression: identification of a unique xenobiotic-responsive element controlling inducible expression by planar aromatic compounds, Proc. Natl. Acad. Sci. USA 87 (1990) 3826–3832.
[9] T. Iyanagi, M. Haniu, K. Sogawa, Y. Fujii-Kuriyama, S. Watanabe, J.E. Shively, K.F. Anan, Cloning and characterization of cDNA encoding 3-methylcholanthrene inducible rat mRNA for UDP-glucuronosyltransferase, J. Biol. Chem. 261 (1986) 15607–15614.
[10] M.S. Denison, S.R. Nagy, Activation of the aryl hydrocarbon receptor by structurally diverse exogenous and endogenous chemicals, Ann. Rev. Pharmacol. Toxicol. 43 (2003) 309–334.
[11] T.A. Gasiewicz, A.S. Kende, G. Rucci, B. Whitney, J. Willey, Analysis of structural requirements for Ah receptor antagonist activity: ellipticines, flavones, and related compounds, Biochem. Pharmacol. 52 (1996) 1787–1803.
[12] E.C. Henry, A.S. Kende, G. Rucci, M.J. Totleben, J. Willey, S.D. Dertinger, R.S. Pollenz, J.P. Jones, T.A. Gasiewicz, Flavone antagonists bind competitively with 2,3,7,8-tetrachlorodibenzo-dioxin (TCDD) to the aryl hydrocarbon receptor but inhibit nuclear uptake and transformation, Mol. Pharmacol. 55 (1999) 716–725.
[13] J.-G. Zhou, E.C. Henry, C.M. Palermo, S.D. Dertinger, T.A. Gasiewicz, Species-specific transcriptional activity of synthetic flavonoids in guinea pig and mouse cells as a result of differential activation of the aryl hydrocarbon receptor to interact with dioxin-responsive elements, Mol. Pharmacol. 63 (2003) 915–924.
[14] S.-H. Kim, E.C. Henry, D.-K. Kim, Y.-H. Kim, K.J. Shin, M.S. Han, T.G. Lee, J.-K. Kang, T.A. Gasiewicz, S.H. Ryu, P.-G. Suh, Novel compound 2-methyl-2 -pyrazole-3-carboxylic acid (2-methyl-4-tolylazo-phenyl)-amide (CH-223191) prevents 2,3,7,8-TCDD-induced toxicity by antagonizing the aryl hydrocarbon receptor, Mol. Pharmacol. 69 (2006) 1871–1878.
[15] A.M. Brzozowski, A.C. Pike, Z. Dauter, R.E. Hubbard, T. Bonn, O. Engstrom, L. Ohman, G.L. Greene, J.A. Gustafsson, M. Carlquist, Molecular basis of agonism and antagonism in the oestrogen receptor, Nature 389 (1997) 753–758.
[16] J. Thompson, D. Higgins, T. Gibson, CLUSTAL W: improving the sensitivity of progressive multiple sequence alignment through sequence weighting, position-specific gap penalties and weight matrix choice, Nuc. Acid Res. 22 (1994) 4673–4680.
[17] M.J. Hartshorn, M.L. Verdonk, G. Chessari, S.C.W. Brewerton, T.M. Mooij, P.N. Mortenson, C.W. Murray, Diverse, high-quality test set for the validation of protein-ligand docking performance, J. Med. Chem. 50 (2007) 726–741.
[18] H. Ashida, I. Fukuda, T. Yamashita, K. Kanazawa, Flavones and flavonols at dietary levels inhibit a transformation of aryl hydrocarbon receptor induced by dioxin, FEBS Lett. 476 (2000) 213–217.
[19] H. Liu, M. Santostefano, Y. Lu, S. Safe, 6-substituted 3,4-benzocoumarins: a new structural class of inducers and inhibitors of CYP1A1-dependent activity, Arch. Biochem. Biophys. 306 (1993) 223–231.
[20] Y. Cheng, W.H. Prusoff, Relationship between the inhibition constant (Ki) and the concentration of inhibitor which causes 50 per cent inhibition (IC_{50}) of an enzymatic reaction, Biochem. Pharmacol. 22 (1973) 3099–3108.
[21] W.H. Bisson, D.C. Koch, E.F. O'Donnell, S.M. Khalil, N.I. Kerkvliet, R.L. Tanguay, R. Abagyan, S.K. Kolluri, Modeling of the aryl hydrocarbon receptor (AhR) ligand binding domain and its utility in virtual ligand screening to predict new AhR ligands, J. Med. Chem. 52 (2009) 5635–5641.